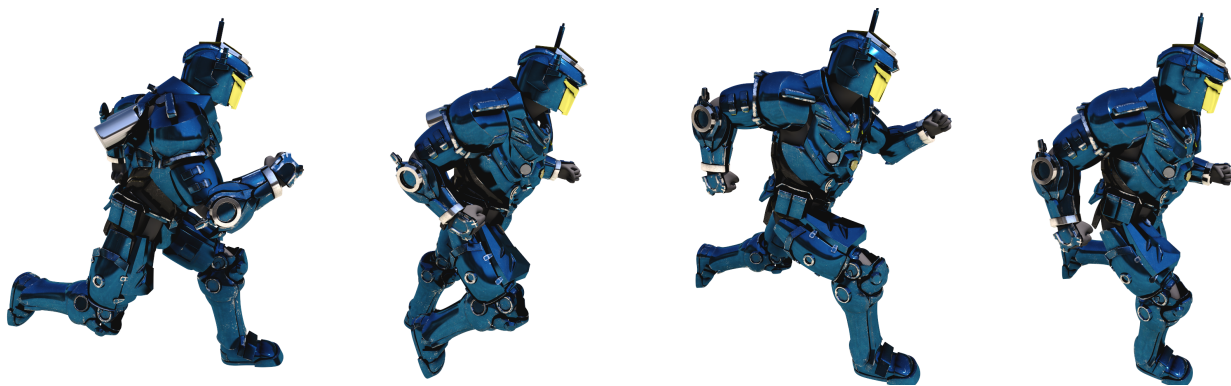


# Massively Parallel Stackless Ray Tracing of Catmull-Clark Subdivision Surfaces

Nikolaus Binder, Alexander Keller

NVIDIA



**Figure 1:** Model composed of Catmull-Clark subdivision surfaces, ray traced with the described direct patch intersection method. Performance:  $\sim 220$  MRays/s for primary and  $\sim 85$  MRays/s for diffuse/reflection rays on an NVIDIA Titan V<sup>TM</sup> GPU. Armor Guy courtesy of © 2014 DigitalFish, Inc. All rights reserved.

## Abstract

We present a fast and efficient method for intersecting rays with Catmull-Clark subdivision surfaces. It takes advantage of the approximation democratized by OpenSubdiv, in which regular patches are represented by tensor product Bézier surfaces and irregular ones are approximated using Gregory patches. Our algorithm operates solely on the original patch data and can process both patch types simultaneously with only a small amount of control flow divergence. Besides introducing an optimized method to determine axis aligned bounding boxes of Gregory patches restricted in the parametric domain, several techniques are introduced that accelerate the recursive subdivision process including stackless operation, efficient work distribution, and control flow optimizations. The algorithm is especially useful for quick turnarounds during patch editing and animation playback.

## 1 Introduction

For many years, Catmull-Clark subdivision surfaces [CC78] have been very popular in feature animation. Besides simple and intuitive modeling, subdivision surfaces facilitate animation because only their control points need to be animated. The original construction has been complemented

by many extensions, such as semi-sharp creases [DKT98] and hierarchically defined detail (multi-resolution surfaces) [PLW97]. Over the recent years OpenSubdiv [Pix12] has been established as the de-facto industry standard for the representation of subdivision surfaces.

While subdivision and evaluation of the parametric surfaces for tessellation of meshes composed from Catmull-Clark subdivision surfaces in a preprocess is well understood and almost trivially integrates into existing ray tracing systems supporting triangle meshes, the incoherent memory access patterns of path tracing and memory constraints on modern graphics hardware are longing for the direct intersection of rays with these surfaces.

## 2 Survey of Previous Work

Rendering systems only computing primary visibility, such as REYES [CCC87] or rasterization, rely on temporary tessellation of subdivision surfaces. Besides using efficient data structures [PS96] or methods to determine tessellated vertices without subdivision [Sta98], the efficiency of this procedure stems from the nature of these systems, which aim to access each surface at most once. In ray tracing based simulations, on the other hand, access is incoherent, and surfaces may be subsequently hit by different generations of rays. While coherency within one generation of rays can be improved by sorting [HKL10], the problem of repeated access across generations remains. Caching the tessellated data allows for a reuse up to a certain degree [BWN<sup>+</sup>15], however the efficiency highly depends on scene complexity, tessellation rate, and cache size. The memory footprint of hierarchies referencing tessellated primitives can be compressed and compactly represented without pointers due to their regular quad-tree structure [SLM<sup>+</sup>16].

In order to display subdivision surfaces at interactive rates, feature adaptive subdivision [NLMD12] determines a set of patches that is submitted to the hardware tessellation units for rasterization. These patches can be partitioned into two classes, regular and irregular patches. Patches are regular unless one of their control points has a valence which is different from four. The limit surface of regular patches can be exactly and efficiently evaluated using cubic tensor product B-Spline or equivalent Bézier surfaces. For the fast evaluation of the limit surface of irregular patches, however, an approximation using Gregory patches [Gre74] is used. As each irregular patch with  $m$  vertices with a valence different from four and  $n$  vertices in total can be subdivided into  $n - m$  regular patches and  $m$  irregular ones, irregular patches are subdivided several times in order to decrease the area in which the approximation is used. A similar refinement is executed for patches next to creases and semi-sharp edges. When tessellating patches, special care has to be taken whenever the subdivision level or tessellation factor differs across edges in order to guarantee crack free surfaces.

Methods that directly determine intersections with subdivision surfaces lend themselves to ray tracing simulations. They neither require parameter tweaking, nor preprocessing, nor additional memory for tessellated geometry and acceleration structures for this micro geometry.

Solutions for the equality of the parametric representation of a ray and those of a surface patch can be computed using root finding of the resulting polynomials using Laguerre’s method [Ral65, Kaj82] or Newton-Raphson solvers [PMS<sup>+</sup>99]. However, methods based on Newton iterations need a good starting point in order to be efficient and to guarantee correct results. While for primary rays these starting points can often be guessed from adjoining rays [JB86], and regions in parameter space with guaranteed convergence of the solver can be identified [Tot85], coherence may lead to incorrect closest intersection points [LG90], only supporting coherent rays is not sufficient, and the cost of identifying safe regions per ray can be prohibitively high in practice. The convergence of Newton iterations can be accelerated by using polynomial extrapolation and by determining better starting points from the bounding volume of the patch defined as a trapezoidal prism [QGGW97], by

adaptively subdividing the patch into parts enclosed in parallelepipeds and referenced by a hierarchy for pruning [BS93], or by simply pre-subdividing patches into smaller ones referenced in the same top-level acceleration data structure [NN12]. Besides improving performance, these methods also improve the quality of starting points, but either increase the memory footprint for the extension of the acceleration structure or add a certain performance overhead.

Recursive subdivision of the patch [Kaj83, Whi80] does not suffer from issues of methods based on root finding. Kobbelt et al. develop a fast on-the-fly subdivision method based on the precomputation of basis functions for the influence of vertices [KDS98]. This, however, needs to be done for all occurring valences and crease values, resulting in a combinatorial explosion. Müller et al. perform adaptive subdivision of the surfaces based on several criteria [MTF03]. Still, the process is elaborate. Testing the projections of the convex hull of the 1-neighborhood can be efficiently performed in a ray centric coordinate system [Woo89], however the resulting bounding volumes are not especially tight. Oriented slabs allow for more accurate pruning of patches than axis aligned bounding boxes, especially for rather flat ones [YSSP91]. Depending on the type of patch and subdivision rules, the effort can be rather low, but may potentially perform redundant computations. Therefore, attempts were made to amortize this cost across groups of rays either by exploiting coherence of primary rays [LG90], by predefining bundles of primary rays [BBLW07], or by sorting batches of rays [HKL10]. As the potential re-use for large scenes, high subdivision depths, and small cache sizes may be small and at the same time the performance of modern massively parallel processors is very fast compared to memory access, subdividing independently for each ray individually is getting more and more interesting. Instead of intersecting with micro geometry, nested hierarchies of axis-aligned bounding boxes of sub-patches determined on demand during recursive subdivision can be refined until the intersected bounding box is sufficiently small to be identified as point of intersection along the ray [PK87, DK06]. The absence of an approximation with false negatives after termination of the subdivision process guarantees watertightness without further effort.

Bézier clipping [NSK90] iteratively reduces the parametric interval in which an intersection can be found by transforming the ray into the parametric  $(u, v)$  space of a patch and cropping it to the bounds of the ray in this space. The original algorithm suffers from several deficiencies that can be resolved [CSS97, EHS05]. It can also be used in conjunction with Newton-Raphson solvers [WSC01]. Tejima et al. combine Bézier clipping with a bi-linear approximation that is used after subdivision termination [TFM15]. While this approximation reduces the number of subdivision steps in flat regions, the approximation with bi-linear surfaces cannot guarantee watertight surfaces: Adjacency on the surface does not necessarily imply shared vertices of the bi-linear approximations. Furthermore, efficient Bézier clipping requires rotations that not only increase the computational cost compared to simple subdivision by bisection, but may also introduce numerical errors visible as cracks in the surface. While consuming patches from an OpenSubdiv preprocess generating Bézier and Gregory patches, their method can only handle tensor product Bézier patches and therefore needs to approximate the approximation with Gregory patches even more. While certain parts are optimized for watertightness, the overall method does not guarantee watertightness: As the final intersection is performed with a bi-linear patch and domain cropping may terminate for different domain sizes, adjacent bi-linear patches do not necessarily meet at connecting edges. Furthermore, precision issues in Bézier clipping may also introduce cracks since the resulting intervals may also suffer from the imprecision due to the initial rotation and all subsequent floating point operations. While the required number of iterations is halved compared to midpoint subdivision, the required effort is significantly higher, especially since midpoint subdivision is extremely cheap and already reduces the parameter interval exponentially.

We also investigate intersecting rays with the bicubic patches generated by OpenSubdiv instead of using them for tessellation, but support both Bézier and Gregory patches and focus on a method

suitable for efficient massive parallelization on GPUs. First, we explain how spatial bounds for both Bézier and Gregory patches can be calculated efficiently for patches cropped to parametric domains. The calculation of spatial bounds for Gregory patches restricted to parametric domains is based on a variant of the algorithm described by Miura et al. [MW94], which we optimize to calculate slightly looser bounds at a reduced cost. Second, these bounds are used for hierarchical culling in an iterative intersection algorithm. Finally, we provide details how performance of our massively parallel implementation can be optimized. With this massive parallelization in mind, stack memory consumption of recursive approaches becomes considerable and may cause bandwidth issues. Therefore, one of the key characteristics of the proposed algorithm is that it does not require a stack for backtracking during subdivision of the patch. Instead, remaining domains are indicated in two bit trails [HL09], kept in registers. Bit trails have previously also been used for backtracking during traversal of bounding volume hierarchies by restarting from the root node [Lai10], by using parent pointers [ÁSK14], or by using a perfect hash map [BK16]. We then calculate control points and/or bounding volumes for remaining domains, whose position and size can be extracted from these bit trails.

### 3 Algorithm

In a pre-process OpenSubdiv performs feature adaptive subdivision on the input mesh to isolate irregular patches and output patch data. Note that we do not need to differentiate between regular and transition patches since we do not need to take special care at boundaries between subdivision levels. After determining conservative spatial bounds of the patches, a hierarchy referencing the patches is built. A ray is then intersected with the mesh by first traversing this hierarchy, pruning patches that cannot be intersected by the ray, and identifying patches potentially intersected by the ray.

In order to determine the first intersection of a ray and a bicubic patch, we partition the parametric unit square recursively, alternating  $u$  and  $v$  direction. Restricting the bicubic patches to the resulting subdomains allows one to determine bounding volumes as derived for Bézier patches in Section 3.1 and Gregory patches in Section 3.2.

Refining the subdomains on demand results in a sequence of nested axis-aligned bounding boxes and in fact intersecting only bounding boxes is sufficient to compute intersections up to almost floating point precision. Section 3.3 details Algorithm 3 that only uses bit trails instead of a stack and recomputes control points for backtracking. The numerical properties of the algorithm are discussed in Section 3.4, and its efficient parallelization is explained in Section 3.5.

#### 3.1 Bounding Bicubic Bézier Patches on Subdomains

A conservative axis aligned bounding box of a bicubic Bézier patch is given by the component-wise minimum and maximum of its control points  $p_{i,j}$  ( $i, j \in \{0, 1, 2, 3\}$ ) as guaranteed by the convex hull property of the tensor product surface.

Sub-patches defined by restricting the parametric domain of a Bézier patch can also be represented by Bézier patches. Control points of a Bézier sub-patch resulting from splitting the domain along a parametric axis can be calculated using de Casteljau subdivision [dC59].

A restriction of a bicubic Bézier patch  $f(u, v)$  defined on the unit square to an arbitrary subdomain  $\mathbb{D} := [u_0, u_1] \times [v_0, v_1] \in [0, 1]^2$  results in a bicubic Bézier patch whose control points as laid out in Figure 2 can be computed by cropping the tensor product surface, for example as implemented in Algorithm 1. Besides intuitively imposing constraints to enforce the properties of the Bézier sub-patch, cropping can be derived by applying de Casteljau subdivision to the patch twice, once

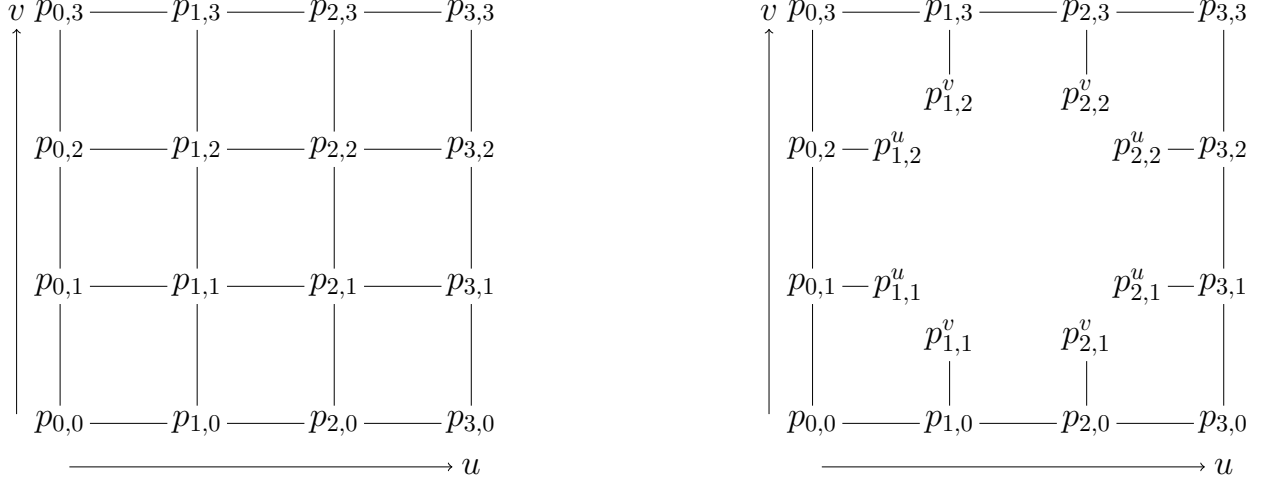


**Figure 2:** Control vertex layout of a bicubic Bézier (left) and Gregory patch (right) along  $u$  and  $v$  direction.

to cut each side of one parametric direction, and repeating the process to crop the other one. In our performance tests, cropping as implemented in Algorithm 1 performed slightly faster than the mathematically equivalent successive cropping of parametric directions.

As splitting a patch using de Causteljau subdivision is significantly faster than computing control points of a sub patch from scratch, we only recompute control points after backtracking, i.e. unless the next domain is a subdomain of the current one.

### 3.2 Bounding Bicubic Gregory Patches on Subdomains

A bicubic Gregory patch is controlled by 20 points as laid out in Figure 2. Given a pair of  $(u, v)$  coordinates, it can be evaluated by reducing it to a bicubic Bézier patch, where the control points on the boundary are identical and the inner control points

$$p_{i,j}(u, v) = g_{i,j}(u, v)p_{i,j}^u + (1 - g_{i,j}(u, v))p_{i,j}^v$$

for  $i, j \in \{1, 2\}$  are determined using the weights

$$g_{i,j}(u, v) = \begin{cases} \frac{v}{u+v} & i = 1, j = 1 \\ \frac{v}{(1-u)+v} & i = 2, j = 1 \\ \frac{(1-v)}{u+(1-v)} & i = 1, j = 2 \\ \frac{(1-v)}{(1-u)+(1-v)} & i = 2, j = 2. \end{cases}$$

Due to the special case  $p_{i,j}^u = p_{i,j}^v = p_{i,j}$ , a Gregory patch may be considered a generalization of a Bézier patch.

While bounding volumes for Gregory patches can also be determined from the convex hull of its control points, determining a bounding volume for the restriction to an arbitrary parametric subdomain  $\mathbb{D} := [u_0, u_1] \times [v_0, v_1] \in [0, 1]^2$  is not as obvious as in the Bézier case, because a subpatch of a Gregory patch may not necessarily be representable as a Gregory patch.

While Gregory patches can be converted to bi-7th degree rational Bézier patches [TOTC90], the approach is ruled out by the additional amount of data, computations, and numerical issues.

However, analyzing the inner control points [MW94] allows for finding bounding volumes of bicubic Gregory patches restricted to  $\mathbb{D}$ : Taking a look at the signs of the derivatives of the weights

$i, j$	$\frac{\partial}{\partial u} g_{i,j}(u, v)$		$\frac{\partial}{\partial v} g_{i,j}(u, v)$	
1, 1	$-\frac{v}{(u+v)^2}$	$\leq 0$	$\frac{u}{(u+v)^2}$	$\geq 0$
2, 1	$\frac{v}{((1-u)+v)^2}$	$\geq 0$	$\frac{1-u}{((1-u)+v)^2}$	$\geq 0$
1, 2	$-\frac{(1-v)}{(u+(1-v))^2}$	$\leq 0$	$-\frac{u}{(u+(1-v))^2}$	$\leq 0$
2, 2	$\frac{(1-v)}{((u-1)+(v-1))^2}$	$\geq 0$	$-\frac{(1-u)}{((u-1)+(v-1))^2}$	$\leq 0$

allows one to bound the weights

$$g_{i,j}^{\min}(\mathbb{D}) := \min_{(u,v) \in \mathbb{D}} g_{i,j}(u, v) = \begin{cases} \frac{u_1}{u_1+v_0} & i = 1, j = 1 \\ \frac{(1-u_0)}{(1-u_0)+v_0} & i = 2, j = 1 \\ \frac{u_1}{u_1+(1-v_1)} & i = 1, j = 2 \\ \frac{(1-u_0)}{(1-u_0)+(1-v_1)} & i = 2, j = 2 \end{cases}$$

and

$$g_{i,j}^{\max}(\mathbb{D}) := \max_{(u,v) \in \mathbb{D}} g_{i,j}(u, v) = \begin{cases} \frac{u_0}{u_0+v_1} & i = 1, j = 1 \\ \frac{(1-u_1)}{(1-u_1)+v_1} & i = 2, j = 1 \\ \frac{u_0}{u_0+(1-v_0)} & i = 1, j = 2 \\ \frac{(1-u_1)}{(1-u_1)+(1-v_0)} & i = 2, j = 2 \end{cases}$$

on the subdomain  $\mathbb{D}$ . Finally, as depicted in Figure 3,

$$\begin{aligned} p_{i,j}^A(\mathbb{D}) &= g_{i,j}^{\min}(\mathbb{D}) p_{i,j}^u + (1 - g_{i,j}^{\min}(\mathbb{D})) p_{i,j}^v, \\ p_{i,j}^B(\mathbb{D}) &= g_{i,j}^{\max}(\mathbb{D}) p_{i,j}^u + (1 - g_{i,j}^{\max}(\mathbb{D})) p_{i,j}^v, \\ p_{i,j}^{\min}(\mathbb{D}) &= \min\{p_{i,j}^A(\mathbb{D}), p_{i,j}^B(\mathbb{D})\}, \text{ and} \\ p_{i,j}^{\max}(\mathbb{D}) &= \max\{p_{i,j}^A(\mathbb{D}), p_{i,j}^B(\mathbb{D})\}, \end{aligned}$$

where minima and maxima are determined component-wise, and hence

$$p_{i,j}^{\min}(\mathbb{D}) \leq p_{i,j}(u, v) \leq p_{i,j}^{\max}(\mathbb{D}) \text{ for } (u, v) \in \mathbb{D}.$$

As obviously  $p_{i,j}^{\min}(\mathbb{D}) = p_{i,j}^{\max}(\mathbb{D}) = p_{i,j}$  for the control points on the patch boundary, the two bicubic Bézier patches defined by the control points on the boundary and  $p_{i,j}^{\min}(\mathbb{D})$  and  $p_{i,j}^{\max}(\mathbb{D})$ , respectively, bound the volume of the restriction of a bicubic Gregory patch to  $\mathbb{D}$ . The bounding volume bounding both bicubic Bézier patches restricted to  $\mathbb{D}$  then bounds the bicubic Gregory patch restricted to  $\mathbb{D}$ .

Instead of maintaining two sets of control points, a conservative bounding volume can be defined by determining the lower bound from the Bézier patch with  $p_{i,j}^{\min}$  as inner control points and extending its upper bound by the maximum displacement vector  $d_{\max}(\mathbb{D})$ , which is defined as the component-wise maximum of the maximal displacements

$$d_{i,j}(\mathbb{D}) := p_{i,j}^{\max}(\mathbb{D}) - p_{i,j}^{\min}(\mathbb{D})$$

of the inner control points.

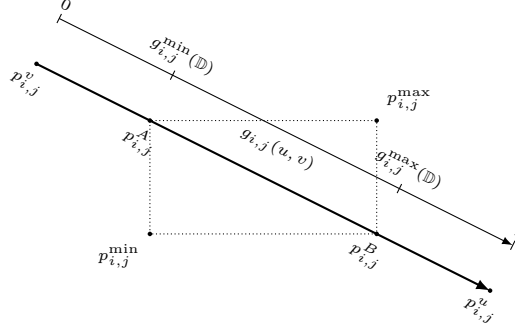


**Figure 3:** Bounding the interpolant  $g_{i,j}(u, v)$  in the domain  $\mathbb{D}$  also bounds the parametric inner control points  $p_{i,j}(u, v)$ .

Unlike the bounding volumes determined by Miura et al. [MW94], we do not use a difference patch based on the  $d_{i,j}$ , but instead derive a conservative upper bound of the displacement of the upper bound, which we will improve in the following:

In floating point arithmetic the displacement is not necessarily monotonously decreasing with increasing subdivision steps and  $\lim_{u_1 \rightarrow u_0, v_1 \rightarrow v_0} d_{\max}(\mathbb{D}) = 0$  cannot be guaranteed. This especially happens when  $u$  and  $v$  are 0 or 1.

The tightness of the bounding volume and its numerical properties can be improved by bounding the tensor product weights

$$w_{i,j}(u, v) = B_i^3(u) \cdot B_j^3(v)$$

in the bicubic Bézier surface formula according to  $\mathbb{D}$ . For example, analyzing the second Bernstein polynomial of degree 3 yields

$$\max_{t_0 \leq t \leq t_1} B_1^3(t) = \begin{cases} \frac{4}{9} & t_0 \leq \frac{2}{3} \wedge t_1 \geq \frac{2}{3} \\ 3 \cdot t_1^2(1 - t_1) & t_1 < \frac{2}{3} \\ 3 \cdot t_0^2(1 - t_0) & t_0 > \frac{2}{3} \end{cases}$$

when restricted to the interval  $[t_0, t_1]$ . A similar bound can be derived for  $B_2^3(t)$  and hence

$$w_{i,j}(u, v) \leq \bar{w}_{i,j}(\mathbb{D}) := \max_{u_0 \leq t \leq u_1} B_i^3(t) \cdot \max_{v_0 \leq t \leq v_1} B_j^3(t)$$

for  $(u, v) \in \mathbb{D}$  and  $i, j \in \{1, 2\}$ . Noting that on the patch boundary  $d_{i,j}(\mathbb{D}) = 0$ , i.e. for  $i, j \in \{0, 3\}$ , the evaluation of a bicubic Bézier patch now can be bounded by

$$\begin{aligned} f(u, v) &= \sum_{0 \leq i, j \leq 3} w_{i,j}(u, v) p_{i,j}(u, v) \\ &\leq \sum_{0 \leq i, j \leq 3} w_{i,j}(u, v) p_{i,j}^{\max}(\mathbb{D}) \\ &= \sum_{0 \leq i, j \leq 3} w_{i,j}(u, v) (p_{i,j}^{\min}(\mathbb{D}) + d_{i,j}(\mathbb{D})) \\ &= \sum_{0 \leq i, j \leq 3} w_{i,j}(u, v) p_{i,j}^{\min}(\mathbb{D}) + \sum_{i, j \in \{1, 2\}} w_{i,j}(u, v) d_{i,j}(\mathbb{D}) \\ &\leq \sum_{0 \leq i, j \leq 3} w_{i,j}(u, v) p_{i,j}^{\min}(\mathbb{D}) + \underbrace{\sum_{i, j \in \{1, 2\}} \bar{w}_{i,j}(\mathbb{D}) d_{i,j}(\mathbb{D})}_{=: d(\mathbb{D})} \end{aligned}$$

Note that  $d(\mathbb{D})$  is now zero in the numerically critical cases ( $u_{0/1}$  and  $v_{0/1}$  are 0 or 1).

Again, in order to bound a bicubic Gregory patch, we first determine the axis-aligned bounding box of the lower bounding Bézier patch, however, now extending it by displacing its upper bound by  $d(\mathbb{D})$ , which includes the bounds on the weights. These computations to determine the control points of the lower bounding Bézier patch and the maximum displacement of the upper bound are subsumed in Algorithm 2.

Now, dealing with both Bézier and Gregory patches can be realized by one unified algorithm (see Algorithm 2), because cropping Bézier patches is simply realized by setting  $d(\mathbb{D})$  to zero and using the inner control points of a Bézier patch instead of calculating  $p_{i,j}^{\min}(\mathbb{D})$ .

### 3.3 Iterative Hierarchical Subdivision

In order to intersect a ray and a parametric patch, we start with the unit square as the parameter domain, which becomes repeatedly partitioned, alternating splits along the  $u$  and  $v$  parameter axes. Instead of an obvious recursive approach, Algorithm 3 traverses the implicit complete binary tree of nested subdomains iteratively.

Therefore both bounding boxes of the two sub-patches resulting from partitioning are intersected with the ray. Avoiding a stack, intersection information now is stored in a bit trail [HL09], one for each parameter. Only if the ray intersects both bounding boxes, the bit corresponding to the current level of subdivision is set in the trail of the current axis to indicate that the second domain also needs to be checked for intersection. Once the bit trail contains only zeros and the current subtree is pruned, traversal is terminated.

Similar to Dammertz et al. [DK06, Sec. 2.1], partitioning can be stopped once the  $L_1$ -norm of the bounding box diagonal projected onto the screen is less than half a pixel width for primary rays. As there is no approximation with a bi-linear surface, flatness criteria are not applicable. After terminating partitioning due to sufficient precision or missing both bounding boxes, the least significant set bit from both trails determines the next domain checked for intersection and the next partition axis. Now, Algorithm 2 determines the inner control points and the maximum displacement  $d$ , and in association with Algorithm 1 re-computes the current set  $p$  of control points for the subdomain specified by position and size as discussed in the previous sections.

Intersecting the two bounding volumes of the sub-patches instead of intersecting only the bounding volume has two main advantages: First, it reduces the frequency of backtracking. Backtracking is expensive compared to de Casteljau subdivision, and can be quite often avoided because one of the two subdomains can immediately be pruned. Second, ordered traversal is as simple as intersecting the sub domain with the closer bounding volume first. While only adding the negligible overhead of comparing hit distances, this ordering helps avoiding the subdivision of hidden parts of patches.

Interestingly, we can use the same subdivision and pruning procedure also for Gregory patches: After subdividing the lower bounding Bézier patch, we extend the maximum bound by the maximum displacement determined on the coarser scale. As the lower bounding Bézier patch of the coarser level also bounds the one on the current level and the maximum displacement is monotonously decreasing, the calculated bounding volumes are conservative.

Our experiments show that the reduction of traversal steps and computation of control points nearly halves traversal time as compared to intersecting only the bounding volume of the patches restricted to the current domain.

We do not calculate the distance to the bounding box  $t_{\text{cur}}$  again on termination, as it has already been determined directly after subdivision. Even if the second domain on the same level was also intersected by the ray, it cannot be closer as the subdomain whose bounding box is closer is checked first. We could therefore also clear the trail bit to avoid backtracking to the same level, but these



cases are so rare that we could not measure any speedup.

For path tracing, we avoid self-intersection by shifting the origin of the subsequent ray along the normal in the intersection by the  $L_1$  distance of the last bounding volume. While this offset is not minimal, it is numerically preferable over the diagonal of the bounding box and always avoids self-intersection.

### 3.4 Numerical Robustness and Watertightness

De Casteljau subdivision is the most robust method for bisection of a Bézier patch as it only performs additions and divisions by two. Intersecting rays with patches using the iterative subdivision method described in Section 3.3 only reports false positives; false negatives can only be introduced by numerical imprecision. In theory, the surface intersected by the algorithm would therefore be completely watertight, and its approximation error would only be an artificial thickness of the patch. It is important to note that this guarantee also includes independence from the local subdivision depth, which clearly differentiates the approach from others using bi-linear approximations after subdivision [BBLW07, TFM15], which either require a fixed subdivision depth or may introduce cracks due to local deviation of subdivision depth.

In practice, special care needs to be taken for intersection of rays with bounding volumes [WBMS05, Ize13]. Furthermore, the recomputation of control points after backtracking may be numerically critical as it may result in control points that differ from the ones calculated by subdivision. An analysis of all included operations may define an upper bound on the deviation which can be used to extend bounding boxes and guarantee watertightness. On the other hand, this deviation can be dramatically reduced by anchoring patches in the origin. In our numerical experiments we measured a deviation as low as 0.0001 %, which suggests that the deviation will most likely be negligible. For some of our meshes the discrepancy between floating point and double precision subdivision is about similar.

Intersecting patches in local frames instead of using world space coordinates for all bounding boxes improves performance significantly by reducing their overlap and therefore lowering the number of parametric domains that cannot be immediately pruned. While the performance often doubles in our test scenes, the transformation to the local frame is a source of numerical precision issues that may become visible as gaps between adjacent patches. Extending bounding boxes at the boundary that fall below a certain size threshold introduces an artificial thickness which closes these gaps.

### 3.5 Efficient Parallelization

The apparent parallelization of the method over rays suffers from very high register pressure: Even for a Bézier patch already 48 registers are required to maintain the set of control points. As the vast majority of calculations is performed component-wise, the number of required registers can be reduced by operating with thread groups of three per ray, using one thread per component of the three-dimensional vectors. Although this approach results in only 30 active threads for a SIMD width of 32 and requires several shuffles of values between threads, our experiments report a speedup of up to 33 %. Besides reducing the register pressure, this parallelization scheme also helps reducing the amount of control flow and data divergence.

In addition, shared state variables can also be maintained across the thread group, which further reduces register pressure and allows for further distributing computations across the thread group. We measure another performance gain of up to 10 % after this optimization.

We also use this parallelization scheme for traversal of the top level hierarchy. While there the number of component-wise computations is relatively low compared to the time spent for memory

```

// ----- one calculation per thread -----
vec3f p0 = 3.0f * a + 2.0f * b + vec3f(12.0f);
vec3f p1 = 1.0f * a - 3.0f * b + vec3f(7.0f);
float best = hmax3(p0) + hmax3(p1);

// ----- in thread groups of three -----
// component wise operations look exactly the same
float p0 = 3.0f * a + 2.0f * b + 12.0f;
float p1 = 1.0f * a - 3.0f * b + 7.0f;
// shuffles required for operations on multiple components
float best = max3(shuffle(p0, lane0),
                  shuffle(p0, lane1),
                  shuffle(p0, lane2)) +
            max3(shuffle(p1, lane0),
                  shuffle(p1, lane1),
                  shuffle(p1, lane2));

```

**Listing 1:** CUDA example for an arbitrary, unrelated calculation using the parallelization scheme using thread groups of three.

access and communication between the threads of a group, we still measured a clear performance advantage over traversal in only one of the three threads of a group and also over a two step method that first traverses the hierarchy with one thread per ray and enqueues ray-patch tuples for a subsequent intersection test. Listing 1 shows an example for a parallelization with this scheme.

Another source of control flow divergence is subdivision, which may split along different parametric directions for different threads of a warp. We avoid this issue completely by transposing the grid of control points after subdivision and after recalculation (if required). This way we only need to split along one parametric direction. As we are only interested in the convex hull of the set of control points, its rotation is irrelevant.

## 4 Results and Discussion

We evaluated the performance of our method using a path tracer with next event estimation on several different generations of NVIDIA GPUs. The numbers presented in this article were obtained using a NVIDIA Titan V<sup>TM</sup>. Due to the simplicity of the models only one primary, one reflection, and one shadow ray to the light sources were traced.

Employing a basic wavefront ray tracer [LKA13], we can distinguish intersection performance from ray setup and shading. We do not perform compaction of the ray stream after intersecting primary rays; intersection performance for secondary rays is therefore not only penalized by increased incoherency of secondary rays, but also by the resulting lower SIMD occupancy.

Intersection performance for larger models is mostly dominated by traversal performance of the hierarchy referencing the patches. We use a simple binary Bounding Volume Hierarchy (BVH), recursively constructed using bins to split approximately according to the Surface Area Heuristic (SAH) [GS87, Hav00, SSK07, Wal07]. Traversal performance can potentially be improved by utilizing spatial splits [SFD09] also for patches. Furthermore, while we traverse a binary hierarchy using a node index stack and persistent threads [AL09], recent advances in stackless BVH traversal [BK16] and fast traversal of wide BVHs on GPUs [YKL17] will certainly also improve the overall performance.

The results in the captions of Figures 1 and 4 show that the direct ray tracing of the bicubic patches resulting from feature adaptive subdivision can be performed interactively or even in real

---

**Algorithm 1: cropBezierPatch:** Calculate control points of a Bézier patch cropped to the parametric domain  $[u_0, u_1] \times [v_0, v_1]$ .

---

**Input:** A Bézier patch defined by its control points  $p$  and the domain  $[u_0, u_1] \times [v_0, v_1]$

**Output:** Control points  $q$  of the cropped Bézier patch

$$\Delta u \leftarrow \frac{u_1 - u_0}{3}$$

$$\Delta v \leftarrow \frac{v_1 - v_0}{3}$$

// Corners

$$q_{0,0} \leftarrow \text{evalBezier}(p, u_0, v_0)$$

$$q_{3,0} \leftarrow \text{evalBezier}(p, u_1, v_0)$$

$$q_{0,3} \leftarrow \text{evalBezier}(p, u_0, v_1)$$

$$q_{3,3} \leftarrow \text{evalBezier}(p, u_1, v_1)$$

// Points on the boundary

$$q_{1,0} \leftarrow q_{0,0} + \Delta u \cdot \text{evalBezierDu}(p, u_0, v_0)$$

$$q_{2,0} \leftarrow q_{3,0} - \Delta u \cdot \text{evalBezierDu}(p, u_1, v_0)$$

$$q_{0,1} \leftarrow q_{0,0} + \Delta v \cdot \text{evalBezierDv}(p, u_0, v_0)$$

$$q_{3,1} \leftarrow q_{3,0} + \Delta v \cdot \text{evalBezierDv}(p, u_1, v_0)$$

$$q_{0,2} \leftarrow q_{0,3} - \Delta v \cdot \text{evalBezierDv}(p, u_0, v_1)$$

$$q_{3,2} \leftarrow q_{3,3} - \Delta v \cdot \text{evalBezierDv}(p, u_1, v_1)$$

$$q_{1,3} \leftarrow q_{0,3} + \Delta u \cdot \text{evalBezierDu}(p, u_0, v_1)$$

$$q_{2,3} \leftarrow q_{3,3} - \Delta u \cdot \text{evalBezierDu}(p, u_1, v_1)$$

// Inner control points

$$\begin{aligned} q_{1,1} \leftarrow & q_{1,0} + \Delta v \cdot \text{evalBezierDv}(p, u_0, v_0) \\ & + \Delta u \cdot \Delta v \cdot \text{evalBezierDuDv}(p, u_0, v_0) \end{aligned}$$

$$\begin{aligned} q_{2,1} \leftarrow & q_{3,1} - \Delta u \cdot \text{evalBezierDu}(p, u_1, v_0) \\ & - \Delta u \cdot \Delta v \cdot \text{evalBezierDuDv}(p, u_1, v_0) \end{aligned}$$

$$\begin{aligned} q_{1,2} \leftarrow & q_{1,3} - \Delta v \cdot \text{evalBezierDv}(p, u_0, v_1) \\ & - \Delta u \cdot \Delta v \cdot \text{evalBezierDuDv}(p, u_0, v_1) \end{aligned}$$

$$\begin{aligned} q_{2,2} \leftarrow & q_{2,3} - \Delta v \cdot \text{evalBezierDv}(p, u_1, v_1) \\ & + \Delta u \cdot \Delta v \cdot \text{evalBezierDuDv}(p, u_1, v_1) \end{aligned}$$

**return**  $q$

---

---

**Algorithm 2: calcPointsAndD:** Calculating control points of a Bézier patch as a lower bound and the maximum displacement of an upper bounding Bézier patch of a Gregory Patch restricted to a domain. For a Bézier patch the lower bounding patch equals the patch itself and the displacement of the upper bound is zero.

---

**Input:** A Bézier/Gregory patch with control points  $p$  and the domain to which it is restricted

$[u_0, u_1] \times [v_0, v_1]$  and a flag *isGregoryPatch*

**Output:** A set of control points  $q$  of the lower bounding Bézier patch and the maximum distance  $d$  of the upper bounding Bézier patch

**if** *isGregoryPatch* **then**

$$\begin{aligned}
p_{1,1}^{min} &\leftarrow \frac{u_0 \cdot p_{1,1}^u + v_1 \cdot p_{1,1}^v}{u_0 + v_1} \\
p_{1,1}^{max} &\leftarrow \frac{u_1 \cdot p_{1,1}^u + v_0 \cdot p_{1,1}^v}{u_1 + v_0} \\
p_{2,1}^{min} &\leftarrow \frac{(1-u_0) \cdot p_{2,1}^u + v_0 \cdot p_{2,1}^v}{(1-u_0) + v_0} \\
p_{2,1}^{max} &\leftarrow \frac{(1-u_1) \cdot p_{2,1}^u + v_1 \cdot p_{2,1}^v}{(1-u_1) + v_1} \\
p_{1,2}^{min} &\leftarrow \frac{u_1 \cdot p_{1,2}^u + (1-v_1) \cdot p_{1,2}^v}{u_1 + (1-v_1)} \\
p_{1,2}^{max} &\leftarrow \frac{u_0 \cdot p_{1,2}^u + (1-v_0) \cdot p_{1,2}^v}{u_0 + (1-v_0)} \\
p_{2,2}^{min} &\leftarrow \frac{(1-u_1) \cdot p_{2,2}^u + (1-v_0) \cdot p_{2,2}^v}{(1-u_1) + (1-v_0)} \\
p_{2,2}^{max} &\leftarrow \frac{(1-u_0) \cdot p_{2,2}^u + (1-v_1) \cdot p_{2,2}^v}{(1-u_0) + (1-v_1)} \\
w_{u,1} &\leftarrow \begin{cases} \frac{1}{3} & u_0 \leq \frac{1}{3} \wedge u_1 \geq \frac{1}{3}, \\ u_1 & u_1 \leq \frac{1}{3}, \\ u_0 & \text{else.} \end{cases} \\
w_{u,2} &\leftarrow \begin{cases} \frac{2}{3} & u_0 \leq \frac{2}{3} \wedge u_1 \geq \frac{2}{3}, \\ u_1 & u_1 < \frac{2}{3}, \\ u_0 & \text{else.} \end{cases} \\
w_{v,1} &\leftarrow \begin{cases} \frac{1}{3} & v_0 \leq \frac{1}{3} \wedge v_1 \geq \frac{1}{3}, \\ v_1 & v_1 < \frac{1}{3}, \\ v_0 & \text{else.} \end{cases} \\
w_{v,2} &\leftarrow \begin{cases} \frac{2}{3} & v_0 \leq \frac{2}{3} \wedge v_1 \geq \frac{2}{3}, \\ v_1 & v_1 < \frac{2}{3}, \\ v_0 & \text{else.} \end{cases} \\
w_{u,1}^{max} &\leftarrow 3 \cdot w_{u,1} \cdot (1 - w_{u,1}) \\
w_{u,2}^{max} &\leftarrow 3 \cdot w_{u,2} \cdot (1 - w_{u,2}) \\
w_{v,1}^{max} &\leftarrow 3 \cdot w_{v,1} \cdot (1 - w_{v,1}) \\
w_{v,2}^{max} &\leftarrow 3 \cdot w_{v,2} \cdot (1 - w_{v,2}) \\
p_{1,1} &\leftarrow \min\{p_{1,1}^{min}, p_{1,1}^{max}\} \\
p_{2,1} &\leftarrow \min\{p_{2,1}^{min}, p_{2,1}^{max}\} \\
p_{1,2} &\leftarrow \min\{p_{1,2}^{min}, p_{1,2}^{max}\} \\
p_{2,2} &\leftarrow \min\{p_{2,2}^{min}, p_{2,2}^{max}\} \\
d &\leftarrow w_{u,1}^{max} \cdot w_{v,1}^{max} \cdot |p_{1,1}^{max} - p_{1,1}^{min}| \\
&\quad + w_{u,2}^{max} \cdot w_{v,1}^{max} \cdot |p_{2,1}^{max} - p_{2,1}^{min}| \\
&\quad + w_{u,1}^{max} \cdot w_{v,2}^{max} \cdot |p_{1,2}^{max} - p_{1,2}^{min}| \\
&\quad + w_{u,2}^{max} \cdot w_{v,2}^{max} \cdot |p_{2,2}^{max} - p_{2,2}^{min}|
\end{aligned}$$

**else**

$d \leftarrow 0$

**end**

$q \leftarrow \text{cropBezierPatch}(p, u_0, u_1, v_0, v_1)$

**return**  $(q, d)$

---

---

**Algorithm 3:** Intersecting a Bézier or Gregory patch.

---

**Input:** A ray with its current closest hit distance  $t_{\max}$ , the patch control points  $p_{\text{org}}$  and a flag  $isGregoryPatch$

**Output:** Intersection details and distance  $t_{\max}$

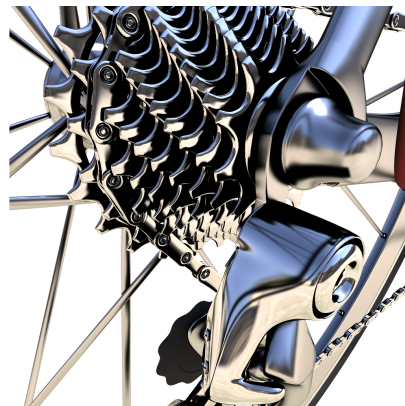
```
pos  $\leftarrow$  (0, 0)
size  $\leftarrow$  ( $2^{23}$ ,  $2^{23}$ )
trail  $\leftarrow$  (0, 0)
axis  $\leftarrow$  0
 $t_{\max} \leftarrow ray.t_{\max}$ 
if  $isGregoryPatch$  then
    | ( $p, d$ )  $\leftarrow$  calcPointsAndD( $isGregoryPatch, p_{\text{org}}, pos, size$ )
else
    |  $p \leftarrow p_{\text{org}}$ 
    |  $d \leftarrow (0, 0, 0)^T$ 
end
while  $true$  do
    | subdividing  $\leftarrow$  false
    | if  $\neg terminate(p, ray, pos, size)$  then
    | | ( $p_L, p_R$ )  $\leftarrow$  subdivideDeCasteljau( $p, axis$ )
    | | ( $hitL, hitR, closest, t_{\text{cur}}$ )  $\leftarrow$  intersect( $ray, t, p_L, p_R, d$ )
    | | if  $hitL$  or  $hitR$  then
    | | | subdividing  $\leftarrow$  true
    | | | size[axis]  $\leftarrow$  size[axis]/2
    | | | if  $hitL$  and  $hitR$  then
    | | | | trail[axis]  $\leftarrow$  trail[axis]  $\oplus$  size[axis]
    | | | end
    | | | if  $closest = R$  or  $\neg hitL$  then
    | | | |  $p \leftarrow p_R$ 
    | | | | pos[axis]  $\leftarrow$  pos[axis]  $\oplus$  size[axis]
    | | | else
    | | | |  $p \leftarrow p_L$ 
    | | | end
    | | | axis  $\leftarrow$  1 - axis
    | | end
    | | else
    | | | if  $t_{\text{cur}} < t_{\max}$  then
    | | | |  $t_{\max} = t_{\text{cur}}$ 
    | | | | intersection  $\leftarrow$  ( $pos, size, \dots$ )
    | | | end
    | | end
    | | if  $\neg subdividing$  then
    | | | if trail = (0, 0) then break
    | | | lvl  $\leftarrow$  countTrailingZeros(trail)
    | | | axis  $\leftarrow$  argmin(lvl)
    | | | if axis = 0 then size  $\leftarrow$  ( $2^{lvl[0]}, 2^{lvl[0]+1}$ )
    | | | else size  $\leftarrow$  ( $2^{lvl[1]}, 2^{lvl[1]}$ )
    | | | pos[axis]  $\leftarrow$  pos[axis]  $\oplus$  size
    | | | trail[axis]  $\leftarrow$  trail[axis]  $\oplus$  size
    | | | pos  $\leftarrow$  pos  $\wedge$   $\neg(size - 1)$ 
    | | | axis  $\leftarrow$  1 - axis
    | | | end
    | | | if  $\neg subdividing$  or  $isGregoryPatch$  then
    | | | | ( $p, d$ )  $\leftarrow$  calcPointsAndD( $isGregoryPatch, p_{\text{org}}, pos, size$ )
    | | | end
    | | end
    | end
return ( $t_{\max}, intersection$ )
```

---



185 Mrays/s (60 Mrays/s)

a) Road Bike (courtesy of Yasutoshi “Mirage” Mori)



73 Mrays/s (51 Mrays/s)

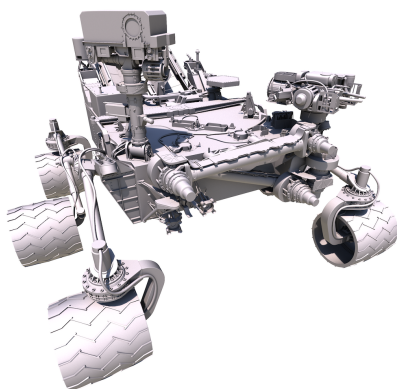


220 Mrays/s (85 Mrays/s)

b) Armor Guy and false color closeup of texture coordinates (courtesy of DigitalFish)

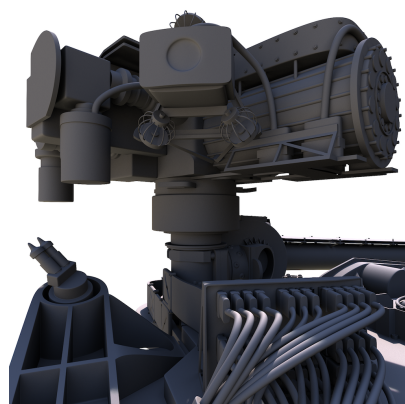


65 Mrays/s (62 Mrays/s)



131 Mrays/s (72 Mrays/s)

c) Curiosity (courtesy of DigitalFish)



70 Mrays/s (43 Mrays/s)

**Figure 4:** Several meshes, ray traced using the described method and the performance for primary (diffuse) rays measured on a NVIDIA Titan V™ GPU.

time. Depending on the scene complexity, the pure intersection performance of pre-tessellated meshes outperforms the presented direct intersection clearly, whereas memory limitations easily can become prohibitive depending on the desired precision. However, taking into account the time required for tessellation and the increased time for bounding volume hierarchy construction, direct intersection in many cases is faster and thus favorable.

## 5 What about Displacements?

Applying displacements to patches complicates the determination of the bounding boxes, as now bounds on both the displacement as well as the range of directions along which the patch is displaced are required.

Bounds on the displacement can be either scalar or vector valued. Efficient lookup requires a hierarchical structure such that the current displacement can be determined with a minimal amount of read operations [Wil83]. Displacement maps can be given per patch [BL08] or in one or multiple textures, which are then accessed using texture coordinates. For the latter bounds cannot be read from a single location in this texture due to a potential warping of the domain. As the size of the hierarchy built for vector valued displacement textures equals the size required for a bounding volume hierarchy of a pre-subdivided patch, using direct intersection with displacements only saves memory if the displacement can be used multiple times, e.g. for motion blur. Depending on their complexity, bounds for procedural displacement of the patch restricted to a parametric domain may be determined quite efficiently [HS98, VAZH<sup>+</sup>09].

While bounds of the possible range of normal directions can be computed using normal cones or tangent cones [MHTAM10], it adds yet another significant overhead.

Displacing a tessellated subdivision surface may remove all mathematical guarantees of the underlying surface. Often, the level of tessellation is selected as level of detail [CFLB06]. While practical in the REYES architecture and rasterization, the visibility may be affected and shadows and silhouettes may be changed [DK06], for example.

The ensemble of these issues raises the interesting question whether a subdivided mesh with a displacement, as used for modeling, is a representation suitable for efficient rendering at all. We therefore see our algorithm as an initial step to start exploring displacements that allow for level of detail and at the same time provide mathematical guarantees for efficient evaluation and visibility error control in future research.

## 6 Conclusion

We have presented a numerically robust algorithm that intersects rays with Bézier and Gregory patches with very high performance and precision on massively parallel hardware based on an improved calculation of bounds of Gregory patches, iterative hierarchical subdivision, and a special parallelization scheme. After creating these patches using feature adaptive subdivision of Catmull-Clark subdivision meshes, they can be efficiently and directly intersected with rays.

Due to the superiority of hierarchical culling over brute force (hardware) tessellation and rasterization, direct ray tracing of these meshes can in some cases even outperform rasterization, which is expected especially for large scenes with a high depth complexity and very high precision requiring fine tessellation for rasterization.

While one might argue about the quality of the approximation of irregular patches by Gregory patches, consistent and thus predictable output from modeling until final rendering may be more important. Hence our new algorithm is beneficial during modeling and animation playback, especially

when caching and tessellation are inefficient and even more so for the large number of applications that do not require displacement.

## References

- [AL09] T. Aila and S. Laine. Understanding the efficiency of ray traversal on gpus. In *Proceedings of the Conference on High Performance Graphics 2009*, HPG '09, pages 145–149, New York, NY, USA, 2009. ACM.
- [ÁSK14] A. Áfra and L. Szirmay-Kalos. Stackless multi-BVH traversal for CPU, MIC and GPU ray tracing. *Computer Graphics Forum*, 33(1):129–140, 2014.
- [BBLW07] C. Benthin, S. Boulos, D. Lacewell, and I. Wald. Packet-based ray tracing of catmull-clark subdivision surfaces. Sci institute technical report uusci-2007-011, University of Utah, 2007.
- [BK16] N. Binder and A. Keller. Efficient stackless hierarchy traversal on gpus with backtracking in constant time. In *Proceedings of High Performance Graphics*, HPG '16, pages 41–50, Aire-la-Ville, Switzerland, Switzerland, 2016. Eurographics Association.
- [BL08] B. Burley and D. Lacewell. Ptex: Per-face texture mapping for production rendering. In *Proceedings of the Nineteenth Eurographics Conference on Rendering*, EGSR '08, pages 1155–1164, Aire-la-Ville, Switzerland, Switzerland, 2008. Eurographics Association.
- [BS93] W. Barth and W. Stürzlinger. Efficient ray tracing for bezier and b-spline surfaces. *Computers & Graphics*, 17(4):423 – 430, 1993.
- [BWN<sup>+</sup>15] C. Benthin, S. Woop, M. Nießner, K. Selgrad, and I. Wald. Efficient ray tracing of subdivision surfaces using tessellation caching. In *Proceedings of the 7th Conference on High-Performance Graphics*, HPG '15, pages 5–12, New York, NY, USA, 2015. ACM.
- [CC78] E. Catmull and J. Clark. Recursively generated B-spline surfaces on arbitrary topological meshes. *Computer-Aided Design*, 10(6):350–355, November 1978.
- [CCC87] R. Cook, L. Carpenter, and E. Catmull. The reyes image rendering architecture. In *Proceedings of the 14th Annual Conference on Computer Graphics and Interactive Techniques*, SIGGRAPH '87, pages 95–102, New York, NY, USA, 1987. ACM.
- [CFLB06] P. Christensen, J. Fong, D. Laur, and D. Batali. Ray tracing for the movie 'Cars'. In *Proc. 2006 IEEE Symposium on Interactive Ray Tracing*, pages 1–6, 2006.
- [CSS97] S. Campagna, P. Slusallek, and H.-P. Seidel. Ray tracing of spline surfaces: Bézier clipping, chebyshev boxing, and bounding volume hierarchy – a critical comparison with new results. *The Visual Computer*, 13(6):265–282, 08 1997.
- [dC59] P. de Casteljau. Outillages methodes calcul. Technical report, Andre Citroen Automobiles SA, Paris, 1959.
- [DK06] H. Dammertz and A. Keller. Improving Ray Tracing Precision by World Space Intersection Computation. In *Proc. 2006 IEEE Symposium on Interactive Ray Tracing*, pages 25–32, Salt Lake City, UT, Sep 2006. IEEE.



- [DKT98] T. DeRose, M. Kass, and T. Truong. Subdivision surfaces in character animation. In *Proceedings of the 25th Annual Conference on Computer Graphics and Interactive Techniques*, SIGGRAPH '98, pages 85–94, New York, NY, USA, 1998. ACM.
- [EHS05] A. Efremov, V. Havran, and H.-P. Seidel. Robust and numerically stable bézier clipping method for ray tracing nurbs surfaces. In *Proceedings of the 21st Spring Conference on Computer Graphics*, SCCG '05, pages 127–135, New York, NY, USA, 2005. ACM.
- [Gre74] J. Gregory. Smooth interpolation without twist constraints. In R. Barnhill and R. Riesenfeld, editors, *Computer Aided Geometric Design*, pages 71–87. Academic Press, 1974.
- [GS87] J. Goldsmith and J. Salmon. Automatic creation of object hierarchies for ray tracing. *Computer Graphics and Applications*, IEEE, 7:14–20, 06 1987.
- [Hav00] Vlastimil Havran. *Heuristic Ray Shooting Algorithms*. Ph.d. thesis, Department of Computer Science and Engineering, Faculty of Electrical Engineering, Czech Technical University in Prague, November 2000.
- [HKL10] J. Hanika, A. Keller, and H. Lensch. Two-level ray tracing with reordering for highly complex scenes. In *Proceedings of Graphics Interface 2010*, GI '10, pages 145–152, Toronto, Ont., Canada, Canada, 2010. Canadian Information Processing Society.
- [HL09] D. Hughes and I. Lim. Kd-jump: a path-preserving stackless traversal for faster isosurface raytracing on GPUs. *Visualization and Computer Graphics*, IEEE Transactions on, 15(6):1555–1562, Nov 2009.
- [HS98] W. Heidrich and H.-P. Seidel. Ray-tracing procedural displacement shaders. In *Proceedings of the Graphics Interface 1998 Conference*, pages 8–16, Vancouver, BC, Canada, June 1998. Canadian Human-Computer Communications Society.
- [Ize13] T. Ize. Robust BVH ray traversal. *Journal of Computer Graphics Techniques (JCGT)*, 2(2):12–27, July 2013.
- [JB86] K. Joy and M. Bhetanabhotla. Ray tracing parametric surface patches utilizing numerical techniques and ray coherence. *SIGGRAPH Comput. Graph.*, 20(4):279–285, August 1986.
- [Kaj82] J. Kajiya. Ray tracing parametric patches. *SIGGRAPH Comput. Graph.*, 16(3):245–254, July 1982.
- [Kaj83] J. Kajiya. New techniques for ray tracing procedurally defined objects. *SIGGRAPH Comput. Graph.*, 17(3):91–102, July 1983.
- [KDS98] L. Kobbelt, K. Daubert, and H.-P. Seidel. Ray tracing of subdivision surfaces. In George Drettakis and Nelson Max, editors, *Rendering Techniques '98*, pages 69–80, Vienna, 1998. Springer Vienna.
- [Lai10] S. Laine. Restart trail for stackless bvh traversal. In *Proceedings of the Conference on High Performance Graphics*, HPG '10, pages 107–111, Aire-la-Ville, Switzerland, Switzerland, 2010. Eurographics Association.

- [LG90] D. Lischinski and J. Gonczarowski. Improved techniques for ray tracing parametric surfaces. *The Visual Computer*, 6(3):134–152, May 1990.
- [LKA13] S. Laine, T. Karras, and T. Aila. Megakernels considered harmful: Wavefront path tracing on gpus. In *Proceedings of the 5th High-Performance Graphics Conference*, HPG '13, pages 137–143, New York, NY, USA, 2013. ACM.
- [MHTAM10] J. Munkberg, J. Hasselgren, R. Toth, and T. Akenine-Möller. Efficient bounding of displaced bézier patches. In *Proceedings of the Conference on High Performance Graphics*, HPG '10, pages 153–162, Aire-la-Ville, Switzerland, Switzerland, 2010. Eurographics Association.
- [MTF03] K. Müller, T. Techmann, and D. Fellner. Adaptive ray tracing of subdivision surfaces. *Computer Graphics Forum*, 22:553–562, 09 2003.
- [MW94] K. Miura and K.-K. Wang. *Ray Tracing Gregory-type Patches*, pages 98–109. World Scientific. Springer-Verlag, Melbourne, Australia, 1994.
- [NLMD12] M. Nießner, C. Loop, M. Meyer, and T. Deroose. Feature-adaptive GPU rendering of Catmull-Clark subdivision surfaces. *ACM Trans. Graph.*, 31(1):6:1–6:11, February 2012.
- [NN12] R. Nigam and P. Narayanan. Hybrid ray tracing and path tracing of bezier surfaces using a mixed hierarchy. In *Proceedings of the Eighth Indian Conference on Computer Vision, Graphics and Image Processing*, ICVGIP '12, pages 35:1–35:8, New York, NY, USA, 2012. ACM.
- [NSK90] T. Nishita, T. Sederberg, and M. Kakimoto. Ray tracing trimmed rational surface patches. In *Proceedings of the 17th Annual Conference on Computer Graphics and Interactive Techniques*, SIGGRAPH '90, pages 337–345, New York, NY, USA, 1990. ACM.
- [Pix12] Pixar. Open Subdiv, <http://graphics.pixar.com/opensubdiv/>, 2012.
- [PK87] R. Pulleyblank and J. Kapenga. The feasibility of a VLSI chip for ray tracing bicubic patches. *Computer Graphics and Applications*, *IEEE*, 7(3):33–44, March 1987.
- [PLW97] K. Pulli, M. Lounsbery, and S. Wa. Hierarchical editing and rendering of subdivision surfaces. Technical Report UW-CSE-97-04-07, University of Washington, Dept. of CS&E, Seattle, WA, 1997.
- [PMS<sup>+</sup>99] S. Parker, W. Martin, P.-P. Sloan, P. Shirley, B. Smits, and C. Hansen. Interactive ray tracing. In *Proceedings of the 1999 Symposium on Interactive 3D Graphics*, I3D '99, pages 119–126, New York, NY, USA, 1999. ACM.
- [PS96] K. Pulli and M. Segal. Fast rendering of subdivision surfaces. In X. Pueyo and P. Schröder, editors, *Rendering Techniques '96*, pages 61–70, Vienna, 1996. Springer Vienna.
- [QGGW97] K. Qin, M. Gong, Y. Guan, and W. Wang. A new method for speeding up ray tracing nurbs surfaces. *Comput. Graph.*, 21(5):577–586, September 1997.

- [Ral65] A. Ralston. *A First Course in Numerical Analysis*. McGraw-Hill, New York City, 1965.
- [SFD09] M. Stich, H. Friedrich, and A. Dietrich. Spatial splits in bounding volume hierarchies. In *Proceedings of the Conference on High Performance Graphics 2009*, HPG '09, pages 7–13, New York, NY, USA, 2009. ACM.
- [SLM<sup>+</sup>16] K. Selgrad, A. Lier, M. Martinek, C. Buchenau, M. Guthe, F. Kranz, H. Schäfer, and M. Stamminger. A compressed representation for ray tracing parametric surfaces. *ACM Trans. Graph.*, 36(1):5:1–5:13, November 2016.
- [SSK07] M. Shevtsov, A. Soupikov, and A. Kapustin. Highly parallel fast kd-tree construction for interactive ray tracing of dynamic scenes. *Comput. Graph. Forum*, 26:395–404, 09 2007.
- [Sta98] J. Stam. Exact evaluation of catmull-clark subdivision surfaces at arbitrary parameter values. In *Proceedings of the 25th Annual Conference on Computer Graphics and Interactive Techniques*, SIGGRAPH '98, pages 395–404, New York, NY, USA, 1998. ACM.
- [TFM15] T. Tejima, M. Fujita, and T. Matsuoka. Direct ray tracing of full-featured subdivision surfaces with bezier clipping. *Journal of Computer Graphics Techniques (JCGT)*, 4(1):69–83, March 2015.
- [Tot85] D. Toth. On ray tracing parametric surfaces. *SIGGRAPH Comput. Graph.*, 19(3):171–179, July 1985.
- [TOTC90] T. Takamura, M. Ohta, H. Toriya, and H. Chiyokura. A method to convert a gregory patch and a rational boundary gregory patch to a rational bézier patch and its applications. In T. Chua and T. Kunii, editors, *CG International '90*, pages 543–562, Tokyo, 1990. Springer Japan.
- [VAZH<sup>+</sup>09] E. Velázquez-Armendáriz, S. Zhao, M. Hašan, B. Walter, and K. Bala. Automatic bounding of programmable shaders for efficient global illumination. *ACM Trans. Graph.*, 28(5):142:1–142:9, December 2009.
- [Wal07] I. Wald. On fast construction of sah-based bounding volume hierarchies. In *Proceedings of the 2007 IEEE Symposium on Interactive Ray Tracing*, RT '07, pages 33–40, Washington, DC, USA, 2007. IEEE Computer Society.
- [WBMS05] A. Williams, S. Barrus, R. Morley, and P. Shirley. An efficient and robust ray-box intersection algorithm. *Journal of Graphics Tools*, 10(1):49–54, 2005.
- [Whi80] T. Whitted. An improved illumination model for shaded display. *Commun. ACM*, 23(6):343–349, June 1980.
- [Wil83] L. Williams. Pyramidal parametrics. *SIGGRAPH Comput. Graph.*, 17(3):1–11, July 1983.
- [Woo89] C. Woodward. Ray tracing parametric surfaces by subdivision in viewing plane. In W. Straßer and H.-P. Seidel, editors, *Theory and Practice of Geometric Modeling*, pages 273–287, Berlin, Heidelberg, 1989. Springer Berlin Heidelberg.

- [WSC01] S. Wang, Z. Shih, and R. Chang. An efficient and stable ray tracing algorithm for parametric surfaces. *Journal of Information Science and Engineering*, 18:541–561, 2001.
- [YKL17] H. Ylitie, T. Karras, and S. Laine. Efficient incoherent ray traversal on gpus through compressed wide bvhs. In *Proceedings of High Performance Graphics*, HPG '17, pages 4:1–4:13, New York, NY, USA, 2017. ACM.
- [YSSP91] J. Yen, S. Spach, M. Smith, and R. Pulleyblank. Parallel boxing in b-spline intersection. *IEEE Computer Graphics and Applications*, 11:72–79, 01 1991.